BJRS

BRAZILIAN JOURNAL
OF
RADIATION SCIENCES
10-03A (2022) 01-13

Radiation shielding for a nuclear fusion device with inertial electrostatic confinement

Lee[1] S.M., Yoriyaz H., Cabral[2] E.L.L.

[1.2] *Instituto de Pesquisas Energéticas e Nucleares /CEENG, 05508-000, São Paulo, SP, Brazil*

[1]*smlee@ipen.br*, [2]*elcabral@ipen.br*

ABSTRACT

In an inertial electrostatic confinement nuclear fusion device, IECF, thermal neutron population is created near the neutron shielding that is proportional to the fast neutrons generation rate; nevertheless, this proportionality varies with the experimental arrangement. Thus, to properly measure the fast neutron generation rate by the IECF device it is necessary to previously elaborate a suitable neutron transport model between the IECF device and the radiation shield, where the neutron detector will be located. This model is elaborated using the Monte Carlo N-Particle Code and the same is used to design the required radiation shield for the safe operation of the device.

Keywords: **IECF, Nuclear Fusion, Radiation Shielding, MCNP6**

ISSN: 2319-0612
DOI: https://doi.org/10.15392/2319-0612.2022.1997
Submitted: 2022-01-31
Accepted: 2022-11-27

1. INTRODUCTION

This work is part of the development of a new type of Inertial Electrostatic Confinement Nuclear Fusion device (IECF) [1-4] and aims to develop a radiation shielding for neutrons and gamma rays generated as result of the fusion reactions and neutron interaction with matters, respectively. Also, this work is to be used for development of a neutron detection system for the IECF device, since neutron detection is essential for the development of a fusion device, due to the fact that obtaining experimental data of the device in operation is required to enable its efficiency analysis and model validation. The first step for detection of the fast neutrons is to slow them down to the thermal state; hence, the radiation shielding for the device must have a moderator material in its composition, enough to assure the thermalization of those neutrons. For these purposes, a transport model is elaborated using the Monte Carlo N-Particle Code (MCNP) [5-7]; which is used to design the required radiation shielding for safe operation of the fusion device; also, it enables the determination of the proportionality between the fast neutrons generated inside the device and the detected thermal neutrons in an arbitrary point. In this context, this work is carried out in two stages: (1) development of a neutron transport model using the MCNP code for simulation of the interaction of the neutrons from fusion reactions with the surrounding materials; and (2) determination of suitable dimensions and materials of the radiation shielding for the IECF device.

2. MATERIALS AND METHODS

For the purpose of the present work, the fusion device is considered as a source of fast neutrons whose production is proportional to fusion reactions inside the IECF. Since the IECF is modeled as a simple cylindrical shell containing deuterium at low pressure, the same is assumed to be a cylindrical, homogeneous, isotropic source of mono-energetic fast neutrons. The energy of neutron is chosen to be 2.5 MeV considering only Deuteron-Deuteron reaction which yields a neutron and a rare isotope of Helium; namely: $D + D \rightarrow {}^{3}He + n + 3.27$ MeV. In this case, neutron and ^{3}He will be released with approximately 2.45 MeV and 0.82MeV, respectively. This fusion reaction is achieved by acceleration of deuterium nuclei in a high voltage between electrodes inside the IECF at low pressure. All the other feasible fusion reaction is ignored for now. The intensity of the neutron source is assumed to be 10^{12} neutrons/sec for the present, but it can vary according to the user's need as well as the neutron energy.

Figure 1 illustrates the model of the laboratory for MCNP simulation, where two radiation barriers inside the room can be observed: a multi-layer box and a shielding shelter.

Figure 1: Layout of the laboratory for MCNP calculation.

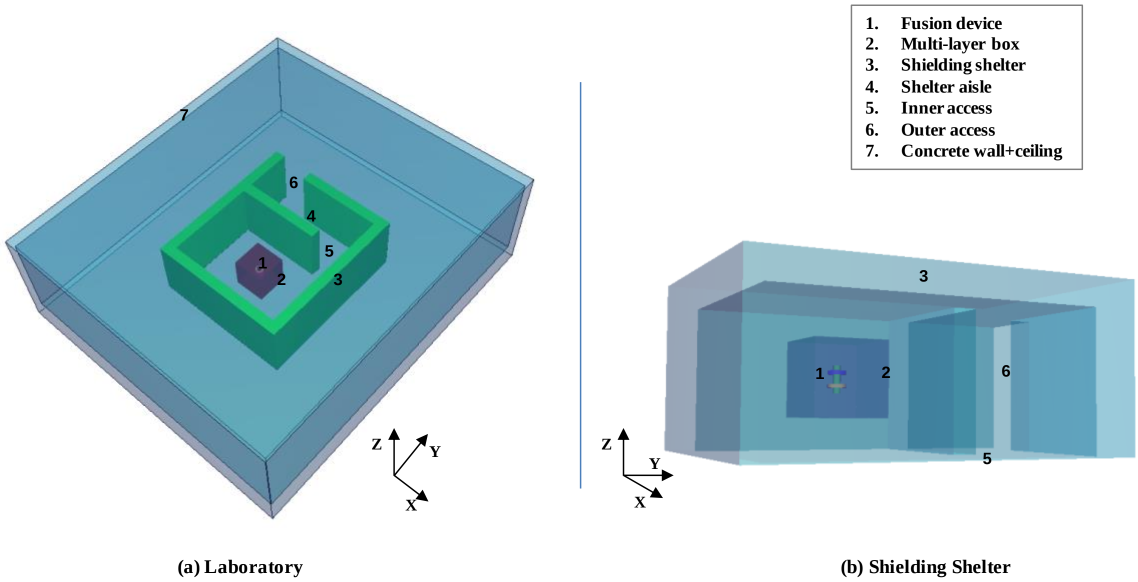

The multi-layer box is the first barrier surrounding the fusion device and composed of three types of materials: 1) neutron moderator; 2) neutron absorber; and 3) structural materials. As the main neutrons moderator, paraffin $C_{31}H_{64}$ (ρ=0,9g/cm^3) is chosen; and as thermal neutron absorber, boric acid, H_3BO_3 (ρ=1,435g/cm3). The density of the main structural material, stainless steel, is assumed to be 7,86g/cm^3. On the other hand, the shielding shelter is mainly for gamma ray attenuation and it consists of a concrete building with density of 2.35 g/cm^3, although simulations are carried out also with shelter of lead (Pb) and of stainless steel for comparison. The width of both inner and outer access of the shelter is 220cm, while the aisle between the accesses is 250cm wide. Figure 2 shows the configuration of a multi-layer box with the IECF inside.

Figure 2: Layout of the small sized multi-layer box for MCNP calculation

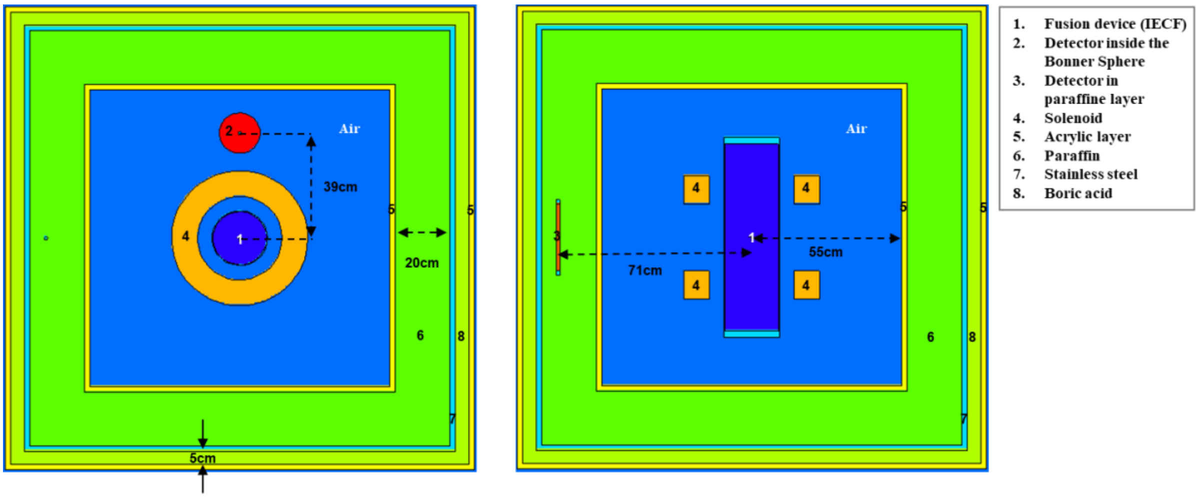

(a) XY-plane (b) XZ-plane

The calculation of radiation doses is performed using the model of an imaginary 850cm radius ring detector, with its origin in the center of the IECF as illustrated in Figure 3. This expedient is a feature of the MCNP code, which is recommended in the code manual [7] for both neutron and gamma rays, mainly in problems with symmetric geometry.

Figure 3: Illustrative image of the ring detector around the shelter.

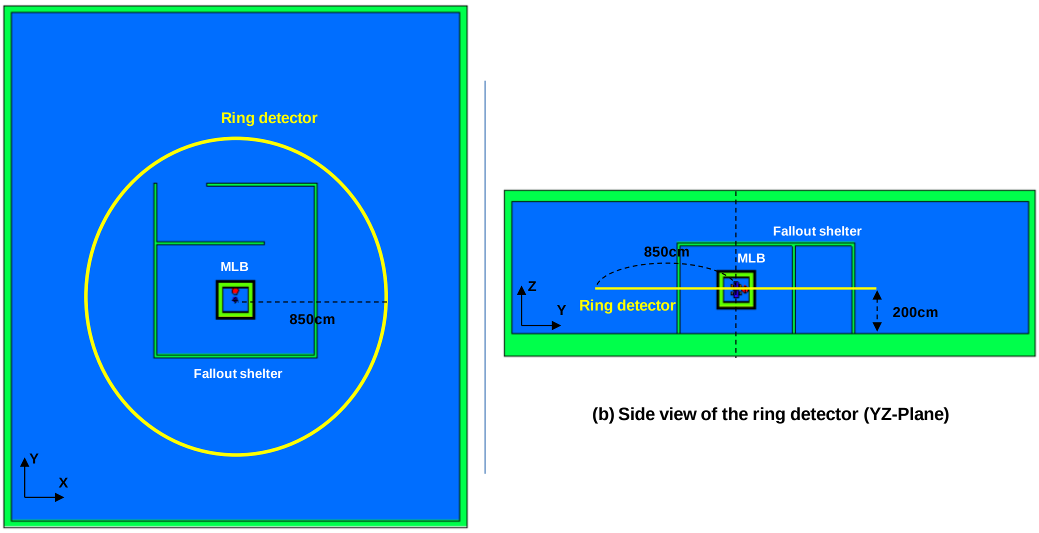

(a) Upper view of the ring detector (XY-Plane)

(b) Side view of the ring detector (YZ-Plane)

Besides the imaginary ring detector, two realistic ^3He proportional neutron detectors are also modeled to estimate the proportionality between the fast neutron generation rate and the thermal neutron count rate in the detection system. Both detectors are identical and cylindrical in shape; one is installed inside the wall of the multi-layer box; while the other is covered by a polyethylene sphere, called a 'Bonner sphere', and positioned in the space between the IECF and the wall of the multi-layer box (MLB). The main dimensions and properties of detectors are:

- Internal diameter/length: 1.27cm /24.892cm;
- External diameter/length: 1.28cm / 28.448 cm;
- Operating voltage: 750 V;
- Internal pressure: 2atm; and
- Sensibility: 7.1 cps/nv

The detectors and the Bonner sphere are illustrated in Figure 4 with their respective dimensions.

Figure 4. Models of (a) an isolated ^3He detector and (b) an identical detector confined within the Bonner sphere. The detector's active region is represented in green.

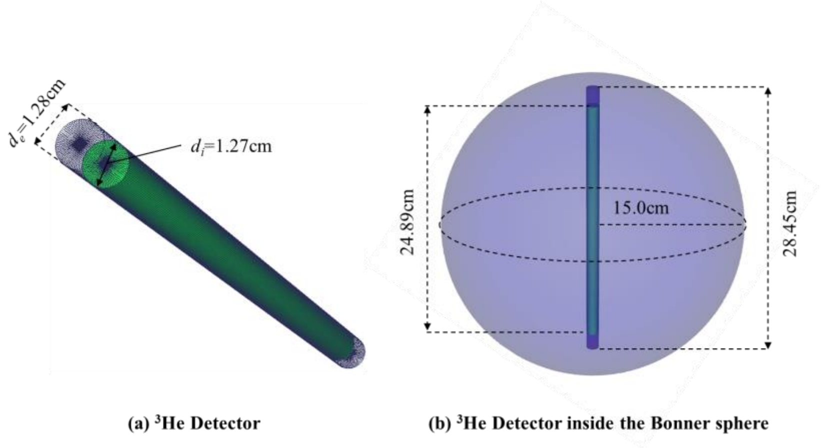

MLB model consists of 5 layers, as shown in Figure 2. Three different sizes of MLB are analysed in this work; the thickness of each configuration are listed in Table I and a closer view of the MLB's cross section is shown in Figure 5.

Table I. The dimensions of the MLB models.

MLB Size	Thickness (cm)					
	Acryl	Paraffin	S Steel	Boric Acid	Acryl	Total
Small	2.0	20.0	2.0	5.0	2.0	31.0
Medium	2.0	24.0	2.0	6.0	2.0	36.0
Large	2.0	30.0	2.0	7.5	2.0	43.5

Figure 5: Cross-sectional view of the multi-layer-box's wall in XY plane.

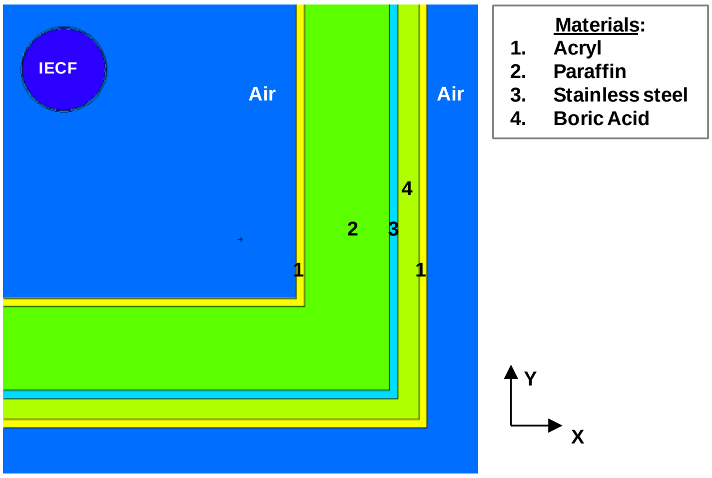

As can be noted in Table I, only the thicknesses of paraffin and boric acid layers vary (denoted by 2 and 4 in Figure 5, respectively), while the acrylic and steel layers (indicated by 1 and 3) are kept constant. The thickenesses of both paraffin and boric acid layers in the medium and large MLBs correspond respectively to 20% and 50% of those of the smallest MLB.

In this way, the average Dose Equivalent along the ring detector surrounding the entire shielding shelter is calculated for each configuration of the MLB varying the thickness of the shelter wall, for each material used for the wall: concrete, lead and steel. In this manner, a search is made for the minimum thickness of the shelter for each material that meets the radiation protection standard.

As the Flux-to-Dose conversion factors for the Dose Equivalent Rate calculation, those of the National Council on Radiation Protection and Measurements, NCRP-38 [7] listed below in Table II, are taken for convenience.

Table II. Neutron Flux-to-Dose Rate Conversion Factors[7].

Energy, E (MeV)	**Flux-to-Dose Rate Conversion Factor, DF(E)** (rem/hr)/(n/cm^2-sec)	**Quality Factor**
2.5E-8	3.67E-6	2,0
1.0E-7	3.67E-6	2,0
1.0E-6	4.46E-6	2,0
1.0E-5	4.54E-6	2,0
1.0E-4	4.18E-6	2,0
1.0E-3	3.72E-6	2,0
1.0E-2	3.56E-6	2,0
1.0E-1	2.17E-5	7,5
5.0E-1	9.26E-5	11,0
1.0	1.32E-4	11,0
2.5	1.25E-4	9,0

Source: American National Standard ANSI/ANS-6.1.1-1977.

3. RESULTS AND DISCUSSION

The neutron and γ-ray Doses Equivalent Rates, DE(n) and DE(γ), calculated with the different combinations of thickness and material of the shielding shelter, for small, medium and large size of MLB are listed in Table III, IV and V, respectively; where the sensitivity of the DE(n) and DE(γ), can be observed with the variation of the thickness of each material for shielding shelter. It can be noticed in the these tables that lead (Pb) is the most effective in reducing the doses caused by γ-rays, as expected; while concrete stands out in neutron shielding in most cases. However, lead is the material that best attenuates the sum of the two doses, DE(n) and DE(γ), as shown in the same tables. This suggests that, when the radiation dose to be shielded in an environment has a considerable neutron contribution with respect to the γ-ray, concrete would be a good choice as a material for the shelter; which is the case of the use of small size multi-layer box (MLB), which allows more neutrons to escape.

Table III. Doses Equivalent Rates using small size MLB.

Material	**Concrete**		**Stainless Steel**		**Lead**	
Shelter wall thickness(cm)	**DE(n) (rem/h)**	**DE(γ) (rem/h)**	**DE(n) (rem/h)**	**DE(γ) (rem/h)**	**DE(n) (rem/h)**	**DE(γ) (rem/h)**
1.0	5,4037E-02	7,0482E-02	5,3557E-02	5,7254E-02	5,5734E-02	4,0860E-02
2.0	5,0483E-02	6,5510E-02	5,0632E-02	4,3488E-02	5,2635E-02	2,5087E-02
3.0	4,7254E-02	6,0652E-02	4,7806E-02	3,3349E-02	5,1730E-02	1,6196E-02
4.0	4,3492E-02	5,5986E-02	4,4217E-02	2,5516E-02	4,9226E-02	1,0015E-02
5.0	3,9861E-02	5,1791E-02	4,1793E-02	1,9823E-02	4,7569E-02	6,4931E-03
6.0	3,6806E-02	4,7781E-02	3,9153E-02	1,5136E-02	4,5972E-02	4,3104E-03
7.0	3,3379E-02	4,4031E-02	3,6643E-02	1,1543E-02	4,5734E-02	2,9085E-03
8.0	3,0688E-02	4,0473E-02	3,3830E-02	8,8421E-03	4,4765E-02	2,0544E-03
9.0	2,8355E-02	3,7353E-02	3,1706E-02	6,9155E-03	4,2615E-02	1,5194E-03
10.0	2,6203E-02	3,4439E-02	2,9244E-02	5,3730E-03	4,0513E-02	1,1647E-03
11.0	2,4101E-02	3,1815E-02	2,6912E-02	4,1878E-03	3,8649E-02	9,6179E-04
12.0	2,2128E-02	2,9401E-02	2,5205E-02	3,2819E-03	3,7881E-02	8,2756E-04
13.0	2,0340E-02	2,7039E-02	2,3421E-02	2,5766E-03	3,6990E-02	7,2801E-04
14.0	1,8654E-02	2,4953E-02	2,1372E-02	2,0613E-03	3,6249E-02	6,8544E-04
15.0	1,6932E-02	2,3077E-02	2,0343E-02	1,6637E-03	3,4199E-02	6,5512E-04

Table IV. Doses Equivalent Rates using medium size MLB

Material	**Concrete**		**Stainless Steel**		**Lead**	
Shelter wall thickness(cm)	**DE(n) (rem/h)**	**DE(γ) (rem/h)**	**DE(n) (rem/h)**	**DE(γ) (rem/h)**	**DE(n) (rem/h)**	**DE(γ) (rem/h)**
1.0	1,6119E-02	5,7362E-02	1,6204E-02	6,1192E-02	1,6695E-02	3,3088E-02
2.0	1,5009E-02	5,3132E-02	1,5025E-02	4,6727E-02	1,5978E-02	2,0131E-02
3.0	1,3797E-02	4,9118E-02	1,4293E-02	3,5272E-02	1,5667E-02	1,2518E-02
4.0	1,2705E-02	4,5436E-02	1,3345E-02	2,6840E-02	1,5001E-02	7,9402E-03
5.0	1,1761E-02	4,1948E-02	1,2623E-02	2,0546E-02	1,4465E-02	5,0611E-03
6.0	1,0767E-02	3,8602E-02	1,1606E-02	1,5713E-02	1,3821E-02	3,1202E-03
7.0	9,9622E-03	3,5545E-02	1,0794E-02	1,2114E-02	1,3451E-02	1,9937E-03

Table V. Doses Equivalent Rates using large size MLB

Material	**Concrete**		**Stainless Steel**		**Lead**	
Shelter wall thickness(cm)	**DE(n) (rem/h)**	**DE(γ) (rem/h)**	**DE(n) (rem/h)**	**DE(γ) (rem/h)**	**DE(n) (rem/h)**	**DE(γ) (rem/h)**
1.0	2,7356E-03	4,2566E-02	2,8016E-03	3,4347E-02	2,9203E-03	2,4631E-02
2.0	2,5387E-03	3,9415E-02	2,4518E-03	2,6321E-02	2,7671E-03	1,5227E-02
3.0	2,3650E-03	3,6405E-02	2,4487E-03	1,9878E-02	2,6792E-03	9,2217E-03
4.0	2,1451E-03	3,3593E-02	2,2293E-03	1,5143E-02	2,4691E-03	5,6973E-03
5.0	1,9831E-03	3,0997E-02	2,1026E-03	1,1586E-02	2,4364E-03	3,5594E-03
6.0	1,8012E-03	2,8482E-02	2,0043E-03	8,8118E-03	2,2376E-03	2,2387E-03
7.0	1,6775E-03	2,6385E-02	1,8952E-03	6,7262E-03	2,2084E-03	1,4006E-03

According to the norm of *Comissão Nacional de Energia Nuclear* (CNEN), the limit of the radiation dose for an individual working in environment with risk of ionizing radiation is 2 rems per year, considering that an operator works 2000 hours cumulatively during this period. Thus, assuming that the IECF device is operated for 10 minutes a day, 5 times a week, for 48 weeks a year; the dose rate limit during the time of experiment would be 0.05 rem/h. Therefore, it can be inferred from Tables III and IV that the minimum thicknesses of the shelter that reduce the total Dose Equivalent to 0.05 rem/h or below are: 13cm for concrete and 7 cm for steel and lead with the small sized MLB (S-MLB) model; while with the medium sized MLB (M-MLB), these thicknesses are reduced to 6cm for concrete and 2cm for steel and lead. On the other hand, Table V shows that, using the large sized MLB (L-MLB) model, the dose is less than 0.05 rem/h in any cases. In other words, the L-MLB by itself meets the CNEN standard without a shelter. The data from Table III, IV and V are graphically represented in Figures 6, 7 and 8, respectively.

Figure 6. Dose Equivalent Rates as a function of concrete thickness, calculated with the S-MLB.

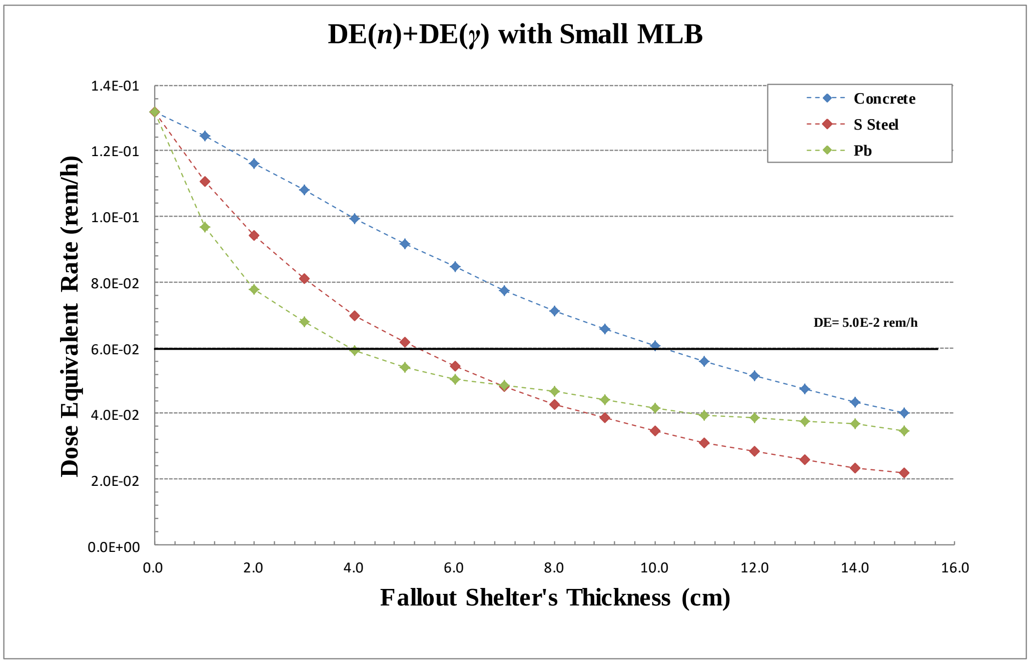

Figure 7. Dose Equivalent Rates as a function of concrete thickness, calculated with the M-MLB.

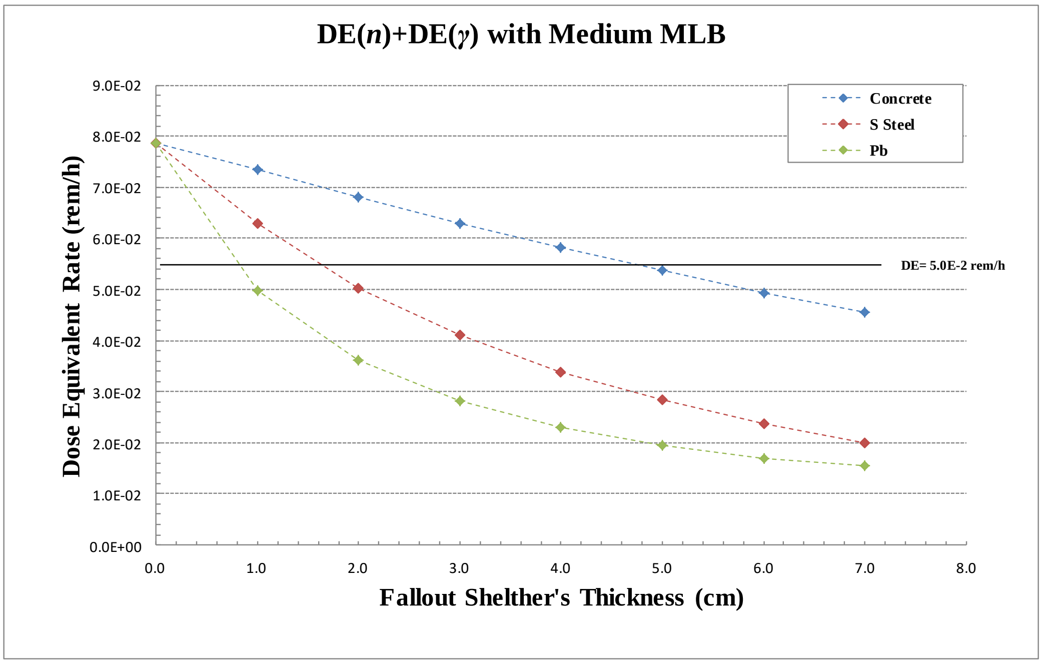

Figure 8. Dose Equivalent Rates as a function of concrete thickness, calculated with the L-MLB.

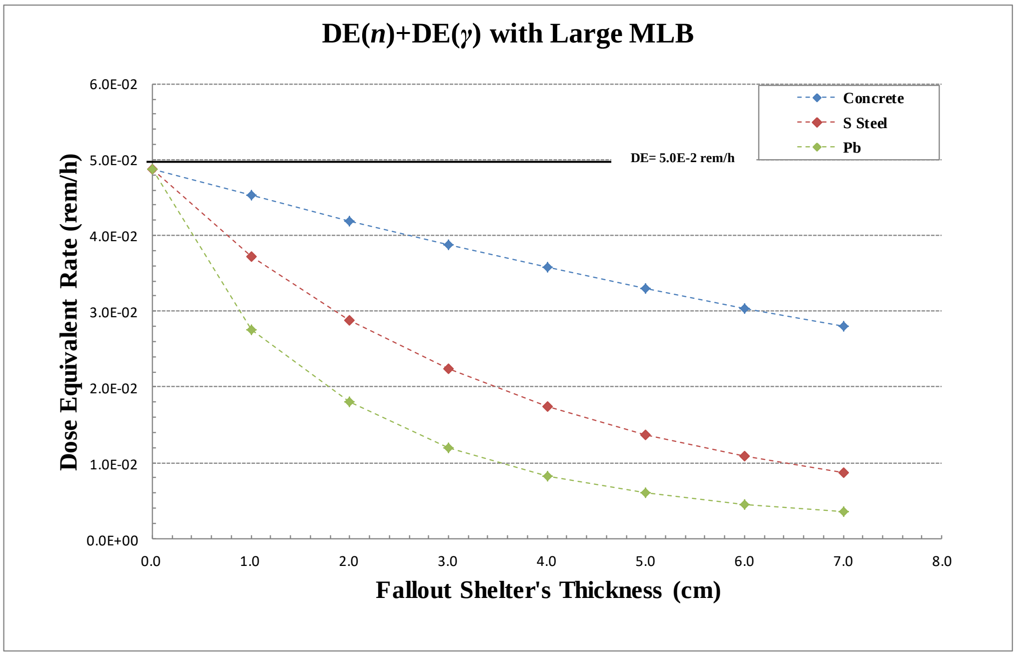

From the Figures 6, 7 and 8 one might conclude that lead is the most appropriate material for shelter wall. Nevertheless, the advantage of lead over stainless steel and concrete in radiation shielding hardly guarantee its eligibility for a shelter construction in most circumstances due to its price, restrictions on purchase and management, malleability, and inappropriateness as main material for a building such as shelter. For example, as shown in Figure 6, the minimum thickness for shelter wall made mainly of lead using the smallest multi-layer-box is around 4 cm, but building and maintaining a lead shelter of wall 4 cm thick would not be a wise move considering the rigidity of the material. In other words, lead could and should be substituted for steel, or even for concrete, practically in most cases.

4. CONCLUSION

Concrete proved to be the most feasible material for shelter, if space is not a concern, not to mention that there are advantages associated with the use of this material for the structure in several aspects. The model used in this work and the obtained results serve as a benchmark for further modeling and experimental studies of radiation shielding for a fusion device, even when there is a need to change the neutron generation rate inside the IECF device, since the results are proportional to the neutron generation rate. Also, even though it is not addressed in this work, the same model can be used for the determination of the proportionality between the fast neutrons generated inside the device and the detected thermal neutrons in an arbitrary point without a significant change in the input file.

ACKNOWLEDGMENT

To Conselho Nacional de Desenvolvimento Científico e Tecnológico (CNPq) for financial support.

The MCNP6 was provided by Prof. Dr. Hélio Yoriyaz, Instituto de Pesquisas Energéticas e Nucleares (IPEN), Brazil.

REFERENCES

[1] R. W. BRUSSARD, **Some Physics considerations of magnetic inertial electrostatic confinement: a new concept for spherical converging-flow fusion**, Fusion Technology, Vol. 19, No. 273. (1991).

[2] W. M. NEVIS, **Can inertial electrostatic confinement work beyond the ion-ion collisional time scale?**, Physics of Plasma, Vol. 2, pp. 1853 (1995).

[3] T. H. RIDER, **A general critique of inertial confinement fusion systems**, Physics of Plasmas, Vol.2 (6) (1995).

[4] M. ROSENBERG AND N. A. KRALL, **The effect of collisions in maintaining a non-Maxwellian plasma distribution in a spherically convergent ion focuses**, Physics of Fluids B, Vol. 4 (1992).

[5] C.J. WERNER, et al., **MCNP6.2 Release Notes**, Los Alamos National Laboratory, Report LA-UR-18-20808 (2018).

[6] C.J. WERNER, **MCNP User’s Manual - Code Version 6.2**, Los Alamos National Laboratory, report LA-UR-17-29981 (2017).

[7] PELOWITZH, DENISE B., et al., MCNP6TM User’s Manual. Version 1.0, Los Alamos National Security, LLC. (2013).